Design of Porous Polymeric Materials from Interpenetrating Polymer Networks (IPNs): Poly(DL-lactide)/Poly(methyl methacrylate)-Based Semi-IPN Systems

Géraldine Rohman, Daniel Grande,* Françoise Lauprêtre, Sylvie Boileau, and Philippe Guérin

Laboratoire de Recherche sur les Polymères, UMR 7581 CNRS-Université Paris XII-Val-de-Marne, 2, rue Henri Dunant, 94320 Thiais, France

Received January 21, 2005; Revised Manuscript Received June 10, 2005

ABSTRACT: Oligoester-containing semiinterpenetrating polymer networks (semi-IPNs) can be effectively used as precursors for the generation of (meso)porous networks with tunable pore sizes. In a first step, novel poly(DL-lactide) (PLA)/poly(methyl methacrylate) (PMMA)-based semi-IPNs were prepared by varying two structural parameters, namely the cross-link density of PMMA subnetwork (initial MMA/dimethacrylate composition ranging from 99/1 to 90/10 mol %) and the cross-linker nature (bisphenol A dimethacrylate, diurethane dimethacrylate). The kinetics of the free-radical cross-linking process was monitored by real-time near-infrared spectroscopy. In a second step, the extraction of the un-cross-linked oligoester subchains from the semi-IPNs was investigated. The possibilities afforded by this straightforward and versatile route to (meso)porous polymeric materials were discussed, and the porosity of the resulting methacrylic networks was examined by scanning electron microscopy (SEM) and thermoporometry using differential scanning calorimetry (DSC). The dependence of pore sizes and pore size distributions on the cross-linker content and nature could be related to turbidity measurements of semi-IPN precursors and explained in terms of polymer−polymer miscibility through the evaluation of PLA/PMMA interaction parameters.

Introduction

Over the past decades, much attention has been paid to the design of porous materials as these systems find a wide array of applications in many areas, including separation and filtration techniques, biomolecule immobilization, controlled drug release, supported catalysis, and template-assisted synthesis of nanomaterials.[1−5] Organic porous materials have unique properties that distinguish them from their inorganic nanostructured analogues, such as mechanical properties that are tunable in a useful range, ability to be functionalized, and higher compatibility with both organic and biological molecules. The basic idea associated with the design of porous polymers generally relies on the introduction of various types of porogens (solvents, gases, small or large molecules) within polymer structures, followed by their selective removal. Gases or solvents used as porogens readily create pores by physically or chemically induced phase separation, resulting in microstructures with broad pore size distributions ranging from micro- and mesopores to macropores (i.e., pore diameters smaller than 2 nm, between 2 and 50 nm, and larger than 50 nm, respectively, according to IUPAC definitions[6]). In contrast, obtaining mesoporous polymeric materials with a well-defined porosity is not a trivial task.

Original approaches toward porous polymers with controlled porosity have used porogen templates able to induce specific structural pores within the residual structures. Miscellaneous porous polymeric materials with uniform pore size distributions that exhibit isotropic or anisotropic morphologies and closed or open pore structures have thus been derived from a large variety of template-oriented routes.[5,7] Some elegant strategies include molecular imprinting,[8,9] removal of self-assembled molecules from supramolecular architectures,[10] selective destruction of one block in self-organized block copolymers,[11−18] and selective thermal or photochemical degradation of a thermoplastic polymer homogeneously blended within a thermostable polymer matrix.[19−21] Even though semidegradable block copolymers are arguably ideal precursors for the formation of ordered mesoporous thin polymeric films, their applicability to the generation of a defined bulk porosity within thicker materials is limited. Moreover, in view of the low mechanical and morphological stability of un-cross-linked polymer structures, approaches based on the use of block copolymers generally require cross-linking of the remaining block.[22]

An alternative and original route to porous cross-linked materials has been put forward through the utilization of (semi)interpenetrating polymer networks (IPNs) as precursors.[23−27] IPNs constitute an intimate combination of two independently cross-linked polymers, at least one being obtained in the immediate presence of the other.[28] Such biphasic polymer structures have been the subject of widespread interest after it was discovered that they may develop microphase-separated cocontinuous morphologies due to their peculiar interlocking framework. Interestingly, if one of the subnetworks is degradable under specific conditions and the other one is stable under these conditions, (meso)porous networks can be designed from such IPNs by resorting to selective degradation methods, e.g., hydrolysis[23−26] or electron beam irradiation.[27]

Although such a straightforward approach has been implemented by a few research groups, the scarcity of literature data on a systematic investigation aiming to establish clear correlations between the structure of the

* Corresponding author: Ph +33 (0)1.49.78.11.77; Fax +33 (0)1.49.78.12.08; e-mail grande@glvt-cnrs.fr.

10.1021/ma0501390 CCC: $30.25
Published on Web 07/29/2005

precursors and the morphology of the resulting porous networks has prompted us to revisit this synthetic strategy. This contribution is the first of a series that thoroughly examines the scope and limitations of utilizing two types of reference systems for the generation of (meso)porous materials. We have specifically chosen semi-IPNs constituted of un-cross-linked oligoesters entrapped in a "rigid" subnetwork as well as IPNs based on an hydrolyzable polyester and a polymer containing a nonhydrolyzable skeleton. The use of polyesters is not coincidental: poly(ϵ-caprolactone) and poly(DL-lactide) (PLA) have been selected because they contain main-chain ester groups that may form favorable dipole−dipole interactions with the side-chain ester groups of a poly(methyl methacrylate) (PMMA) subnetwork and lead to an increase of the compatibility between the two partners in semi-IPNs and IPNs.

In the present paper, we first describe the preparation of novel PLA/PMMA-based semi-IPNs by varying two structural parameters, namely the cross-link density of the PMMA subnetwork and the nature of the cross-linker. The influence of both parameters on the kinetics of the free-radical copolymerization process involved in network formation is carefully examined by real-time near-infrared spectroscopy. Porous methacrylic networks are then derived from mere extraction of linear PLA oligomers from the semi-IPNs. Pore sizes and pore size distributions are determined by scanning electron microscopy (SEM) and thermoporometry via differential scanning calorimetry (DSC) measurements. The dependence of pore sizes on the cross-linker content and nature can be related to turbidity measurements of the semi-IPN precursors and interpreted in terms of polymer−polymer miscibility in such precursors.

Experimental Section

Materials. Dihydroxy-telechelic PLA (M_n (^{1}H NMR) = 1700 g mol^{-1}; M_w/M_n (SEC) = 1.2) was synthesized by ring-opening polymerization of DL-lactide initiated by the ethylene glycol/tin(II) octanoate system according to a literature method.[29] The DSC thermogram exhibited the typical behavior of an amorphous oligomer with a well-defined glass transition temperature (T_g) at 15 °C. Methyl methacrylate (MMA, Aldrich) was distilled under vacuum prior to use. Bisphenol A dimethacrylate (BADMA) and diurethane dimethacrylate (DUDMA) were purchased from Aldrich and used as received. AIBN (Merck) was purified by recrystallization from methanol.

Preparation of PMMA Single Networks. Typically, a single network with a MMA/DUDMA molar composition of 90/10 mol % was prepared as follows. A homogeneous mixture of MMA (0.9 g, 9 mmol), DUDMA (0.47 g, 1 mmol), and AIBN (0.033 g, 0.2 mmol) was degassed under vacuum and poured under nitrogen into a mold which consisted of two glass plates clamped together and separated by a 2 mm thick silicone rubber gasket. The mold was then kept at 65 °C for 2 h, and the reaction medium was finally cured at 110 °C for 2 h. To remove and determine the sol fraction, the resulting network was subjected to a Soxhlet extraction with dichloromethane for 24 h. After extraction, the sample was dried under vacuum and weighed in order to calculate the sol fraction (mass percentage of extractables).

Preparation of PLA/PMMA Semi-IPNs. A standard synthesis of a semi-IPN with a PLA/PMMA mass composition of 50/50 wt % and a MMA/DUDMA molar composition of 90/10 mol % is described next. 0.50 g of PLA, 0.33 g (3.3×10^{-3} mol) of MMA, 0.17 g (3.6×10^{-4} mol) of DUDMA, and 12 mg (7.3×10^{-5} mol) of AIBN ($[AIBN]_0/([MMA]_0 + 2[DUDMA]_0) = 0.02$) were mixed homogeneously in a flask and degassed under vacuum. The solution was introduced under nitrogen into a mold which consisted of two glass plates clamped together and separated by a 2 mm thick silicone rubber gasket. The mold was then placed in an oven operating at 65 °C. After 2 h, the temperature was raised to 110 °C for a 2 h curing.

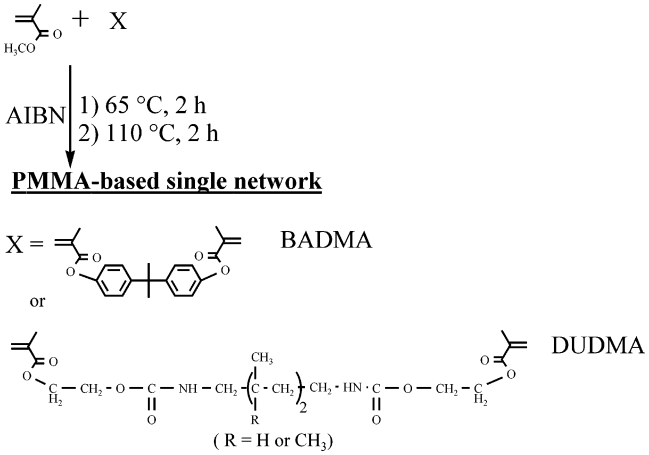

Figure 1. Preparation of PMMA-based single networks.

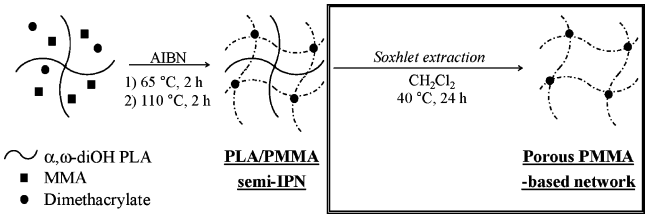

Figure 2. Synthesis of PLA/PMMA-based semi-IPNs and design of porous PMMA networks derived therefrom.

Other single networks and semi-IPNs were synthesized in similar ways by changing the dimethacrylate nature (DUDMA or BADMA) and/or the initial MMA/dimethacrylate molar ratio (90/10, 97/3, 95/5, or 99/1 mol %), as depicted in Figures 1 and 2, respectively.

Formation of Porous Networks by Extraction from Semi-IPNs. PLA/PMMA semi-IPNs were extracted for 24 h at 40 °C in a Soxhlet apparatus with dichloromethane. The recovered sol fractions (after removing the solvent using a rotary evaporator) and extracted networks were dried under vacuum and weighed prior to further analyses. The extraction of linear PLA oligomers from semi-IPNs thus led to the formation of residual porous PMMA networks (Figure 2).

Instrumentation. ^{1}H NMR spectra of sol fractions were recorded at room temperature using a Bruker AC 200 spectrometer operating at a resonance frequency of 200 MHz. The sample concentration was 10 mg mL^{-1}, and $CDCl_3$ was used as the solvent and internal standard (7.27 ppm). High-resolution solid-state ^{13}C NMR spectra of networks were obtained at a resonance frequency of 75 MHz on a Bruker Avance 300 spectrometer using the combined techniques of cross-polarization (CP), dipolar decoupling (DD), and magic angle spinning (MAS). A 4 mm MAS head probe was used with a spinning frequency of 6500 Hz.

The size exclusion chromatography (SEC) equipment comprised a Spectra Physics P100 pump, two PLgel 5 μm mixed-C columns (Polymer Laboratories), and a Shodex RI 71 refractive index detector. Tetrahydrofuran (THF) was used as the eluent at a flow rate of 1 mL min^{-1}, and polystyrene standards (Polymer Laboratories) were employed for calibration.

DSC analyses were carried out with a Perkin-Elmer DSC 4 calorimeter under a nitrogen atmosphere. All samples were scanned twice from −50 to 200 °C at a heating rate of 20 °C min^{-1}, the second run being recorded after quenching. No noticeable degradation was detected under such conditions. The T_g values were measured in the second run: to determine a T_g range, the lower ($T_{g,onset}$) and upper ($T_{g,end}$) limits were identified as the values associated with the intercepts of tangent to midpoint of the specific heat increment with "glassy" and "viscous" baselines, respectively.

Scanning electron microscopy (SEM) analyses were performed with a LEO 1530 microscope equipped with a high-vacuum (10^{-10} mmHg) Gemini column. The accelerating tensions ranged from 1 to 5 kV; two types of detectors (InLens and Secondary Electron) were used. Prior to analyses, the samples were cryofractured and coated with a Pd/Au alloy (4 nm) in a Cressington 208 HR sputter-coater.

Kinetic Studies by Real-Time FTIR Spectroscopy. In the kinetics studies, the FTIR spectra were recorded on a Bruker Tensor 27 DTGS spectrometer between 6500 and 450 cm^{-1} by averaging 32 consecutive scans with a resolution of 4 cm^{-1}. Scan accumulations were repeated every minute for the first 20 min and then every 5 min for the remaining time.

In the case of PMMA single networks and PLA/PMMA semi-IPNs, the network formation kinetics could be monitored in real time in the near-infrared spectral region through the disappearance of the C=C overtone absorption band from the methacrylate groups at 6168 cm^{-1}. Prior to the analyses, the validity of the Beer−Lambert law was checked in the concentration and temperature ranges used in this work. The band intensity being directly proportional to the monomer concentration, the conversion−time profiles can be readily derived from the FTIR spectra recorded as a function of time. Indeed, from the initial absorbance value A_0 and that at a given time A_t, the relative conversion of C=C double bond can be determined as $p = 1 - A_t/A_0$. No thickness correction was needed, thanks to the geometry of the sample cell. Indeed, the latter was maintained vertically, thus preventing thickness variation during the reactions.

The mixture of all reagents was injected into an IR cell which was built for each experiment. A glass-window cell with a 1 mm thick Teflon gasket was used to record the conversion of methacrylate groups, as the corresponding overtone absorption is situated in the near-infrared. The cell was fixed into a solid holder that was placed in an electrical heating jacket equipped with an automatic temperature controller (Specac). The temperature of the block was constant within ±1 °C of the set temperature.

Turbidimetry by UV−Vis Spectroscopy. The turbidity τ of a semi-IPN sample, before extraction, was determined from the measurement of its transmittance Tr at 460 nm (networks do not absorb at this wavelength) by using a Perkin-Elmer model 554 UV/vis spectrophotometer. The τ value was calculated according to the Beer−Lambert extinction law (eq 1) as follows:

$$\tau\ (\mathrm{mm}^{-1}) = \frac{-\ln(Tr)}{e} \tag{1}$$

where e is the sample thickness (2 mm). For a minimal Tr value of 0.001, the corresponding limit value of τ is equal to 3.45 mm^{-1}.

In a pioneering study,[30] Blundell et al. determined the mean size of PMMA spherical domains embedded in a continuous matrix of cross-linked polyurethane by turbidimetry. It should be pointed out that Blundell's theory can also be applied to nonspherical domains. Therefore, the average size of PLA domains associated with the disperse phase within the PMMA matrix in our semi-IPN samples could be assessed from turbidity measurements. Thus, the τ value led to the calculation of the parameter $B(y)$ as shown in eq 2:

$$\tau = \frac{2\pi\phi(1-\phi)(\Delta n)^2 B(y)}{\lambda n^2} \tag{2}$$

where λ, ϕ, and n are the wavelength used, the volume fraction of PLA, and its refractive index, respectively. The difference in refractive indices of phases, Δn, was determined from the difference of the values measured for pure PLA oligomer and PMMA network samples. The n values were measured at the wavelength of the sodium D ray ($\lambda_0 = 589$ nm) using a Prolabo refractometer connected to a thermostated bath operating at 25 °C.

Then, the parameter y was derived from the resolution of eq 3:

$$B(y) = \left[\frac{y^2+2}{y}\right]\left[\frac{y^2+2}{y^2+1} - \frac{2}{y^2}\ln(y^2+1)\right] \tag{3}$$

The average equivalent diameter L_{PLA} of PLA microdomains was finally obtained from eq 4:

$$L_{\mathrm{PLA}}\ (\mathrm{nm}) = \frac{\lambda y}{4\pi(1-\phi)} \tag{4}$$

Thermoporometry by DSC. Thermoporometry is a quantitative technique for determining pore size and pore size distribution in porous materials through DSC analyses. It relies on the melting temperature (T_m) depression and the Gibbs−Thompson effect shown by a solvent constrained within the pores.[31]

As a matter of fact, from the melting thermograms of water contained in the porous methacrylic networks, the T_m depression could be correlated to the pore diameter D_p as indicated by eq 5:[31a,c]

$$D_{\mathrm{p}}\ (\mathrm{nm}) = 2\left(0.68 - \frac{32.33}{T_{\mathrm{m}} - T_{\mathrm{m0}}}\right) \tag{5}$$

where T_m and T_{m0} are the melting temperatures of confined and bulk water, respectively.

The pore size distribution dV/dR vs D_p could be derived from the melting thermograms by using eq 6:[31a,c]

$$\mathrm{d}V/\mathrm{d}R\ (\mathrm{cm}^3\ \mathrm{nm}^{-1}\ \mathrm{g}^{-1}) = \frac{\mathrm{d}q/\mathrm{d}t(T_{\mathrm{m}} - T_{\mathrm{m0}})^2}{32.33\rho v m \Delta H(T)} \tag{6}$$

where dq/dt, ρ, v, m, and $\Delta H(T)$ are the heat flow recovered by DSC, the water density, the heating rate, the sample mass, and the melting enthalpy of water, respectively. $\Delta H(T)$ was calculated from eq 7:[31a,c]

$$\Delta H(T)\ (\mathrm{J}\ \mathrm{g}^{-1}) = 332 + 11.39(T_{\mathrm{m}} - T_{\mathrm{m0}}) + 0.155(T_{\mathrm{m}} - T_{\mathrm{m0}})^2 \tag{7}$$

To increase the hydrophily of the porous PMMA networks and facilitate the penetration of water into their pores, the samples were first immersed in ethanol for 2 h. After this treatment, deionized water was gradually added to remove the ethanol. The samples were placed for 1 h in ethanol/water mixtures of different volume compositions (70/30, 50/50, 30/70 vol %), and they were then immersed in pure water for 1 week. After wiping, the melting thermograms were recorded from −50 to 5 °C at a heating rate of 1 °C min^{-1}.

Results and Discussion

1. Preparation and Characterization of PMMA Single Networks. As a starting point for our synthetic studies, PMMA-based single networks were prepared as model systems by bulk free-radical copolymerization of MMA with a dimethacrylate using AIBN as the initiator, at 65 °C for 2 h, followed by a 2 h curing process at 110 °C. Two different difunctional cross-linkers were employed: BADMA, a "rigid" dimethacrylate, and DUDMA, a "softer" one. The influence of cross-link density on the structure and properties of the resulting networks was also probed by varying the initial dimethacrylate content from 1 to 10 mol %. All networks were subjected to a CH_2Cl_2 extraction for 24 h at 40 °C. As expected, they were transparent, before and after extraction, and the amounts of sol fractions are reported in Table 1. It is noteworthy that the extractable contents were below 5 wt % in all instances,

Table 1. Sol Fractions (wt %) and Visual Aspects Associated with PMMA Single Networks and PLA/PMMA (50/50 wt %) Semi-IPNs[a]

initial MMA/dimethacrylate composition (mol %)	single network		semi-IPN	
	BADMA	DUDMA	BADMA	DUDMA
90/10	5 (tr)	3 (tr)	62 (o)	51 (tl)
95/5	3 (tr)	1 (tr)	62 (o)	51 (tr)
97/3	3 (tr)	1 (tr)	58 (tl)	59 (tr)
99/1	2 (tr)	< 1 (tr)	50 (tr)	50 (tr)

[a] Experimental conditions: $[AIBN]_0/([MMA]_0 + 2[dimethacrylate]_0) = 0.02$, 2 h at 65 °C + 2 h at 110 °C. o = opaque, tl = translucent, tr = transparent.

indicating a near completion of the cross-linking processes. ^{1}H NMR and SEC analyses showed that the sol fractions were essentially constituted of PMMA oligomers ($M_n \approx 980$ g mol^{-1}; $M_w/M_n \approx 1.6$). Moreover, for DUDMA-based systems, traces of unreacted MMA and/or dimethacrylate were detected only when using an initial 10 mol % content of dimethacrylate. As for BADMA-derivatized systems, the content of residual methacrylate compounds was slightly higher and increased with BADMA content (cf. section 3). The relatively low curing temperature compared to the network T_g may account for such results.

The T_g values of all extracted single networks as determined by DSC are listed in Table 2. DUDMA-based networks exhibited fairly narrow glass transition ranges, and hardly any variation of the T_g ranges with the dimethacrylate content was noticed. Actually, when increasing the cross-link density, the rigidifying effect might be offset by the relatively "softness" of DUDMA that contains a flexible spacer between the two methacrylate groups. Concerning the networks cross-linked by BADMA, the onset of T_g was very close to that determined for DUDMA-based homologues, except for the 10 mol % BADMA-containing sample. However, broad glass transition ranges were observed: the higher the BADMA content, the broader the T_g zone. Such wide distributions of polymer chain mobility may be attributed to a substantial extent of structural heterogeneity in the three-dimensional systems due to the coexistence of PMMA subchains, rigid BADMA cross-links, and even pendent C=C double bonds in the case of 5 and 10 mol % dimethacrylate contents, as detected by FTIR (attenuated total reflection (ATR) mode) at 1640 cm^{-1}. In the latter case, the curing temperature (110 °C) was not high enough compared to the T_g range, which did not allow for an effective and complete copolymerization process,[32] as shown by real-time FTIR (cf. section 3). It should be mentioned that the curing temperature of network formation was not raised beyond 110 °C because of thermal degradation of PLA oligomers at higher temperatures, during the synthesis of the corresponding PLA/PMMA semi-IPNs. Thermogravimetric analysis under a nitrogen atmosphere indeed showed that the decomposition of PLA oligomers begins at 115 °C.

2. Synthesis and Characterization of PLA/PMMA Semi-IPNs. Various PLA/PMMA (50/50 wt %) semi-IPNs were prepared by bulk free-radical copolymerization of MMA and a dimethacrylate (BADMA or DUDMA) with different compositions, in the presence of PLA oligomers, under experimental conditions identical to those employed for single network preparation. The semi-IPN samples were extracted in a Soxhlet with CH_2Cl_2 for 24 h, and the amounts of sol fractions are reported in Table 1. Regardless of the dimethacrylate nature and content, the extraction of linear PLA oligomers was quantitative, as indicated by extractable contents higher than or equal to 50 wt %. No undesired grafting of PLA subchains onto PMMA subnetworks through transfer reactions was detected in the present systems. The total disappearance of the characteristic bands associated with α,ω-dihydroxy-PLA oligomer (hydroxyl and carbonyl groups) in the FTIR (ATR mode) and solid-state ^{13}C NMR spectra of semi-IPNs after extraction confirmed the latter assertion. Furthermore, ^{1}H NMR and SEC analyses of sol fractions gave evidence that not only initial PLA oligomer but also PMMA oligomers (4−10%; $M_n \approx 1000$ g mol^{-1}; $M_w/M_n \approx 1.6$) were recovered. A higher dimethacrylate content in the PMMA subnetwork was mostly associated with an increase in the proportion of PMMA oligomers. This may be ascribed to a reactivity of the cross-linker higher than that of MMA and to an earlier gelation of the reaction medium in the presence of increasing amounts of cross-linker (cf. section 3). No residual MMA or dimethacrylate was detected in these systems, as confirmed by the complete disappearance of the C=C absorption band at 1640 cm^{-1} in the FTIR spectra.

DUDMA-based semi-IPN samples, before extraction, displayed single and fairly narrow glass transition ranges (Table 2). The T_g values were quite low and comprised between the T_g of PLA oligomer (15 °C) and those of corresponding PMMA single networks. Yet, the T_g ranges of semi-IPNs did not match the values calculated from the Fox equation for miscible blends. The transparent or translucent aspect of these semi-IPN samples solely argued in favor of the absence of phase separation at a length scale of a few hundreds of nanometers (cf. Table 1 and section 4). Actually, because of the presence of favorable weak interactions between PLA subchains and PMMA subnetworks, the T_g ranges could well be fitted by the values calculated from the Gordon−Taylor equation ($T_g^b = T_g^1 + k(\omega_2/\omega_1)(T_g^2 - T_g^b)$, where ω_i refers to the mass fractions, 1, 2, and b denote PLA, PMMA, and the blend, respectively, and $k = 0.25$), as previously shown for PLA/PMMA miscible blends.[33] Moreover, up to a 5 mol % initial content of DUDMA, the values of the heat capacity jump at the glass transition (ΔC_p) were in good agreement with that of a 50/50 wt % physical blend constituted of PLA oligomer ($\Delta C_{p,PLA} = 0.55$ J g^{-1} °C^{-1}) and PMMA-prepared under experimental conditions identical to those employed for single network preparation ($\Delta C_{p,PMMA} = 0.2$ J g^{-1} °C^{-1}). Indeed, the ΔC_p value found for such a miscible blend was 0.33 J g^{-1} °C^{-1} with a T_g ranging from 27 to 50 °C.

The situation is more complicated in the case of BADMA-derivatized semi-IPNs before extraction (Table 2). For a 1 mol % initial content of dimethacrylate, its behavior was similar to that observed for its DUDMA-based homologues, in accordance with its transparent aspect (Table 1). In contrast, BADMA-containing semi-IPNs with an initial dimethacrylate content higher than or equal to 5 mol % were opaque, suggesting a length scale of phase separation larger than a few hundreds of nanometers. Therefore, the narrow glass transition ranges exhibited by such samples probably corresponded to PLA-rich domains, as the low T_g values measured could not be fitted by the Gordon−Taylor equation mentioned above. The corresponding ΔC_p values were much lower than that of the miscible PLA/PMMA blend.

Table 2. DSC Analysis of PMMA Single Networks and PLA/PMMA (50/50 wt %) Semi-IPNs

initial MMA/dimethacrylate composition (mol %)	single network after extraction			semi-IPN before extraction			semi-IPN after extraction		
	$T_{g,onset}$ (°C)	ΔT_g[a] (°C)	ΔC_p[b] (J g^{-1} °C^{-1})	$T_{g,onset}$ (°C)	ΔT_g[a] (°C)	ΔC_p[b] (J g^{-1} °C^{-1})	$T_{g,onset}$ (°C)	ΔT_g[a] (°C)	ΔC_p[b] (J g^{-1} °C^{-1})
MMA/BA DMA									
90/10	76	90	0.12	19	11	0.24	134	33	0.12
95/5	114	54	0.20	20	10	0.21	96	63	0.24
97/3	116	29	0.20	27	17	0.22	124	19	0.21
99/1	119	18	0.24	16	38	0.33	113	33	0.25
MMA/DUDMA									
90/10	118	19	0.16	25	18	0.23	116	27	0.19
95/5	114	16	0.16	24	30	0.29	116	20	0.17
97/3	110	23	0.19	23	27	0.35	109	21	0.18
99/1	111	23	0.21	23	23	0.34	110	20	0.18

[a] $\Delta T_g = T_{g,end} - T_{g,onset}$: range of temperatures in which the glass transition occurs as determined by DSC. [b] $\Delta C_p = C_{p,v} - C_{p,g}$: heat capacity jump at T_g as determined by DSC, where C_p is the heat capacity and the subscripts v and g refer to the "viscous" and "glassy" states, respectively.

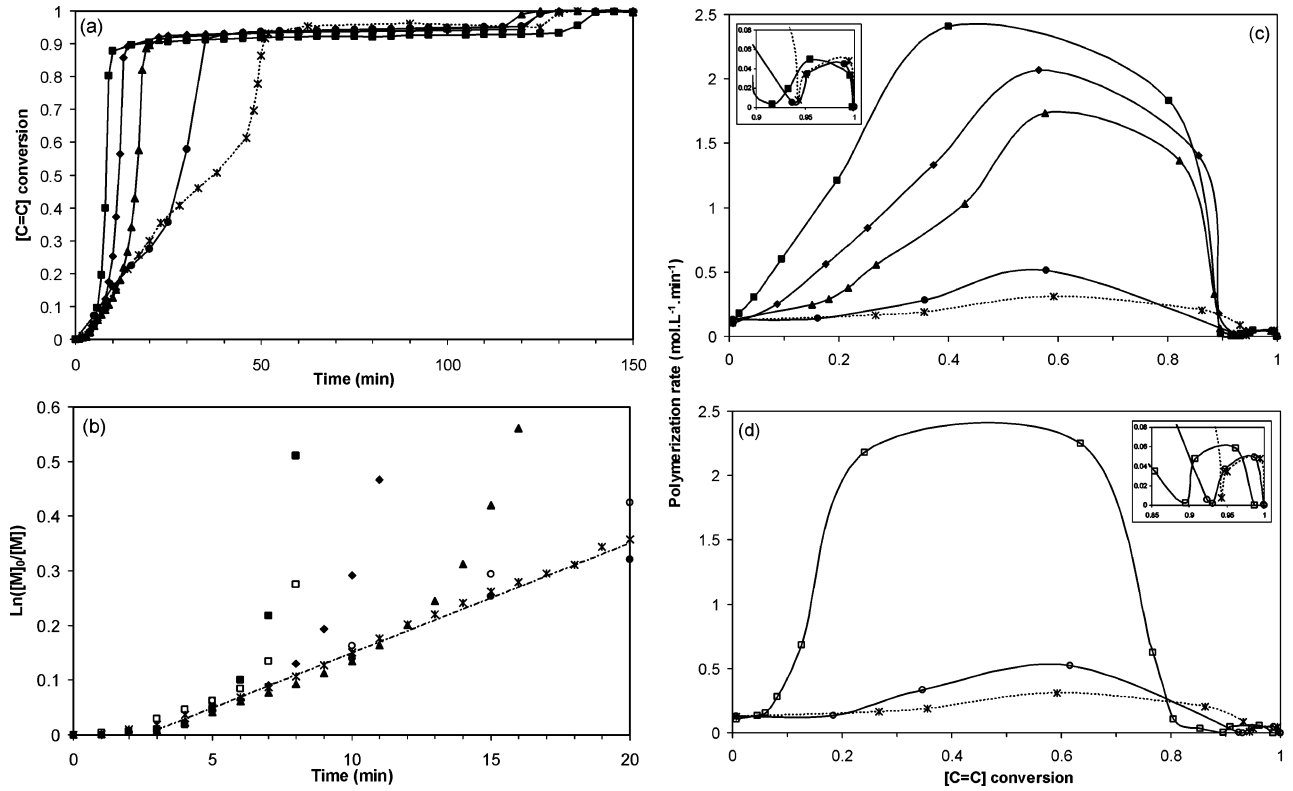

Figure 3. Influence of the dimethacrylate nature and content on PMMA single network formation with $[AIBN]_0/[M]_0 = 0.02$: (a) conversion−time plots for DUDMA-containing systems; (b) $\ln([M]_0/[M])$−time curves for DUDMA- (full symbols) and BADMA-containing (empty symbols) systems; polymerization rate−conversion curves for (c) DUDMA- and (d) BADMA-containing systems with different initial MMA/dimethacrylate compositions: (■, □) 90/10 mol %; (◆) 95/5 mol %; (▲) 97/3 mol %; (●, ○) 99/1 mol %; (∗) 100/0 mol %.

It may be presumed that the upper T_g values related to PMMA-rich domains could not be detected under the DSC conditions used, probably due to their cross-linked nature. These results strongly indicate a substantial heterogeneity of composition in PLA/PMMA semi-IPNs with initial BADMA contents higher than 3 mol %. It is most noteworthy that the T_g and ΔC_p values of semi-IPNs, after extraction, matched those of the corresponding single networks pretty well. This arises from the quantitative extraction of PLA oligomers.

3. Kinetics of Single Network and Semi-IPN Formation by Real-Time FTIR. Jin et al.[34] have investigated the kinetics of formation of polyurethane/PMMA IPNs by FTIR spectroscopy, and the C=C stretching band at 1639 cm^{-1} was used to monitor the formation of the PMMA subnetwork. In our investigation, the C=C absorption band from both MMA and dimethacrylates at 1640 cm^{-1} mostly overlaps the intense and relatively broad C=O stretching bands from PMMA and PLA. Consequently, to monitor the network formation kinetics, we chose a well-separated absorption band, namely, the C=C overtone band of methacrylate groups located in the near-infrared spectral region at 6168 cm^{-1}. This type of band was previously selected to determine the time dependence of the double bond conversion for the cross-linking of diethylene glycol bisallyl carbonate (CR39).[35,36]

Single Network Formation. We first examined the influence of the dimethacrylate content and nature on the kinetics of the free-radical copolymerization process involved in the formation of PMMA single networks. Conversion−time curves are shown in Figure 3a for the DUDMA/MMA system, while the dependence of the polymerization rate (R_p)—determined from the slope of

each point of the latter curves—on conversion is plotted in Figure 3c,d for both DUDMA/MMA and BADMA/MMA systems. As the dimethacrylate content was varied from 0 to 10 mol %, the conversion−time curves were shifted toward shorter times, thus showing an acceleration of the polymerization process. Whatever the dimethacrylate content, the conversion profiles exhibited three main phases with distinct durations. After a 2−3 min induction period, a rather short step (10−50 min depending on the dimethacrylate content) characterized by a rapid consumption of (co)monomers up to 85−95% conversion occurred. Then, a second stage took place up to 120 min of reaction, during which conversion built up very slowly or came to a standstill. Finally, the conversion increased up to completion upon raising the temperature to 110 °C. These kinetic features confirmed that the curing process was effective enough to ensure a quantitative cross-linking in most cases, even though the temperature used in this work (110 °C) was slightly lower than the T_g values of the networks.

At the beginning of the free-radical copolymerization processes (Figure 3b), a close inspection of the variations of $\ln([M]_0/[M])$ vs time clearly showed that the dimethacrylate content had no effect on the initial R_p, as an identical slope was found for the linear parts of the curves. This slope actually matched that obtained for the homopolymerization of MMA. Obviously, the linear parts corresponded to the steady-state regime, and its duration depended on the dimethacrylate content: the higher the cross-linker content, the shorter the steady-state regime (5−20 min for 10−1 mol % DUDMA, respectively). The partial linearity of $\ln([M]_0/[M])$ vs time gave evidence that the internal order of the reactions with respect to monomer was equal to 1. From the slope of the linear parts of the plots, we determined a value of the apparent rate constant (k_{app}) for the copolymerization process of MMA with DUDMA at 65 °C ($k_{app} = k_p(2f k_d/k_t)^{1/2}$, where f stands for the initiator efficiency and k_p, k_d, and k_t are rate constants of propagation, initiator decomposition, and termination, respectively): $k_{app} = (3.8 \pm 0.9) \times 10^{-2}$ L$^{1/2}$ mol$^{-1/2}$ min^{-1}. It is interesting to point out that this value is in good agreement with that calculated from literature data[37] for the bulk free-radical homopolymerization of MMA at 65 °C, i.e., 3.4×10^{-2} L$^{1/2}$ mol$^{-1/2}$ min^{-1}. The $\ln([M]_0/[M])$−time curves then departed from linearity due to the occurrence of the Trommsdorff effect. This effect is typically encountered in a bulk free-radical process and results from an important viscosity increase in the reaction medium; the polymerization is first autoaccelerated, and the polymerization rate then slows down to zero. Figure 3c,d shows that the maximum polymerization rate was advanced and dramatically increased with dimethacrylate content. In fact, increasing amounts of cross-linker induced an earlier onset and a higher intensity of the Trommsdorff effect. Interestingly, upon raising the temperature to 110 °C, the remaining AIBN was rapidly decomposed, and the polymerization resumed with a minor Trommsdorff effect. Most of the systems could reach complete conversion.

Semi-IPN Formation. Next in our investigation, the kinetics of the cross-linking process involved in the formation of PLA/PMMA semi-IPNs was examined. The variations of $\ln([M]_0/[M])$ with time and polymerization rate with conversion for the copolymerization of MMA with different contents of either DUDMA or BADMA

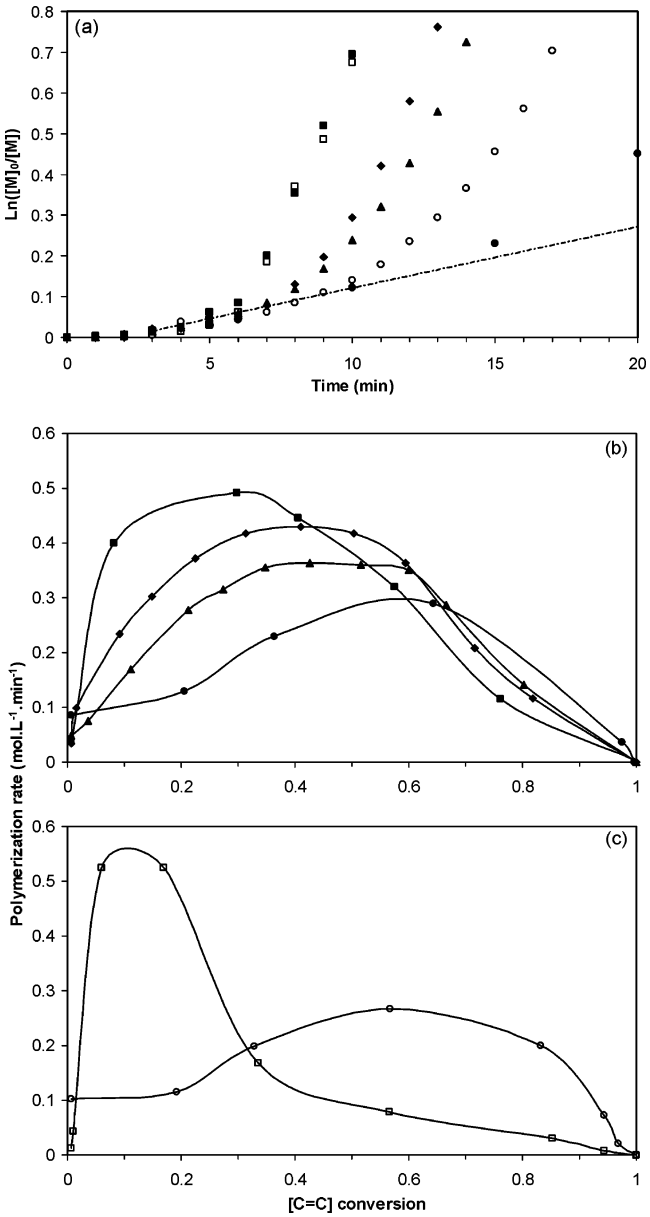

Figure 4. Influence of the dimethacrylate nature and content on PLA/PMMA (50/50 wt %) semi-IPN formation at 65 °C and $[AIBN]_0/[M]_0 = 0.02$: (a) $\ln([M]_0/[M])$−time curves for DUDMA- (full symbols) and BADMA-containing (empty symbols) systems; polymerization rate−conversion curves for (b) DUDMA- and (c) BADMA-containing systems with different initial MMA/dimethacrylate compositions: (■, □) 90/10 mol %; (◆) 95/5 mol %; (▲) 97/3 mol %; (●, ○) 99/1 mol %.

are plotted in Figure 4. Unlike the PMMA single network formation, the conversion profiles just displayed two main phases: after a 2−3 min induction period and the relatively short stage characterized by a rather fast consumption of comonomers (20−60 min depending on the dimethacrylate content and nature), the second period occurred during which conversion built up slowly to completion before the temperature was raised to 110 °C. At the onset of the free-radical copolymerization processes (t < 10 min), the variations of $\ln([M]_0/[M])$ with time were linear, indicating that the internal order of the reactions with respect to monomer was again equal to 1. However, in comparison with the formation of corresponding single networks, the duration of the steady-state regime was shortened, and the maximum polymerization rates were much more ad-

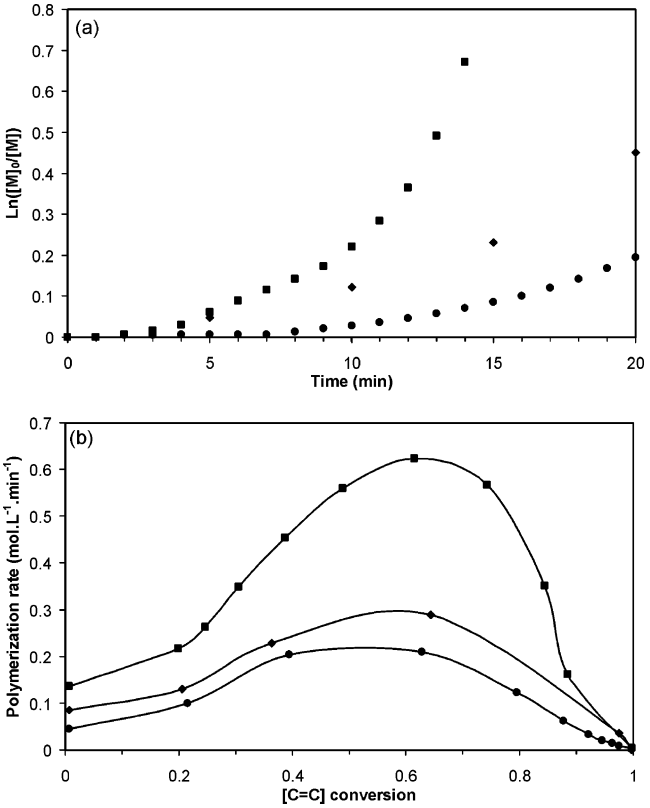

Figure 5. Influence of the AIBN concentration on PLA/PMMA (50/50 wt %) semi-IPN formation with an initial MMA/DUDMA composition of 99/1 mol %: (a) $\ln([M]_0/[M])$−time curves, (b) polymerization rate−conversion plots with different $[AIBN]_0/[M]_0$ ratios: (■) 0.05; (◆) 0.02; (●) 0.005.

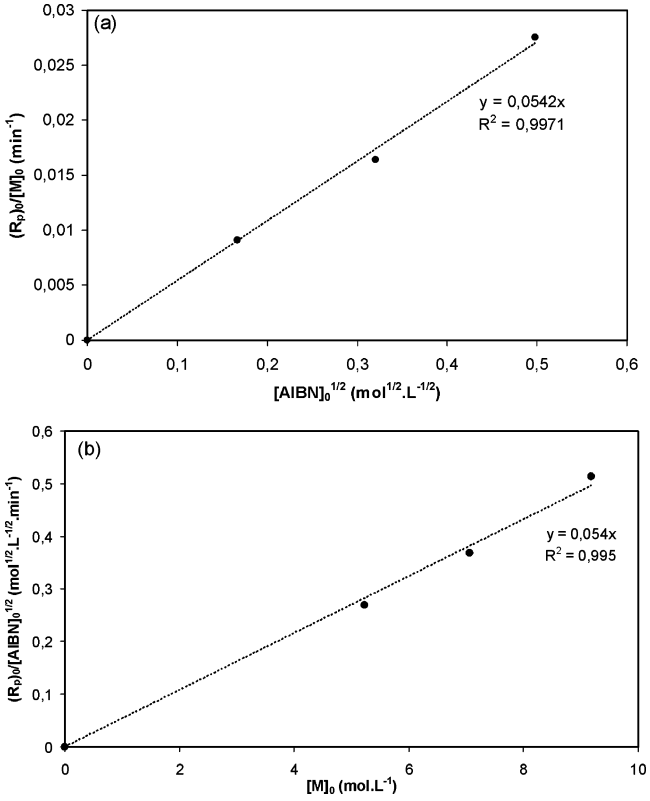

Figure 6. Plots of (a) $(R_p)_0/[M]_0 = f([AIBN]_0^{1/2})$ and (b) $(R_p)_0/[AIBN]_0^{1/2} = f([M]_0)$ for MMA/DUDMA copolymerization at 65 °C with an initial MMA/DUDMA composition of 99/1 mol % in PLA/PMMA semi-IPN formation.

vanced and damped, especially at higher dimethacrylate contents. Because of its viscosity, the presence of PLA oligomer caused an acceleration of the gelation at a lower conversion: such a viscous compound indeed induced an earlier onset of the Trommsdorff effect with a lower intensity, as previously shown by Widmaier.[34] To account for such differences in single network and semi-IPN formations, we also needed to direct our attention to the glass transitions of the systems. As a matter of fact, the "soft" oligoester behaved rather like a diluent toward the methacrylic copolymerization process, preventing the reaction medium from attaining the glassy state as a solvent would have done it. As the temperature of the reaction medium, i.e. 65 °C, was above the T_g values of semi-IPN systems, the process could proceed to complete conversion. In light of these kinetic features, the curing process at 110 °C turned out to be useless in semi-IPN formation; nevertheless, its occurrence allowed semi-IPN samples to possess the same thermal history as that of the corresponding single networks. As a reminder, the curing process was carried out at a temperature below that associated with the onset of the decomposition of PLA oligomers.

To determine the order of the reaction with respect to initiator and the apparent rate constant for the MMA/DUDMA copolymerization process in the presence of PLA oligomers, at 65 °C, we varied the initial molar ratio of initiator to monomer ($[AIBN]_0/[M]_0$, $[M]_0 = [MMA]_0 + 2[DUDMA]_0$) from 0.5 to 5 mol % for the 1 mol % DUDMA-containing semi-IPN system (Figure 5). As expected, the polymerization was faster when increasing AIBN concentration. The initial and maximum R_p increased with increasing $[AIBN]_0$ on account of higher concentrations of free radicals. At the beginning of the polymerization process, the steady-state regime was obeyed, and the linear variation of the $(R_p)_0/[M]_0$ vs $[AIBN]_0^{1/2}$ curve (Figure 6a) showed that the order of the reaction with respect to AIBN was equal to 0.5. From the slope of this curve, we determined a k_{app} value of $(5.4 \pm 1.0) \times 10^{-2}$ $L^{1/2}$ $mol^{-1/2}$ min^{-1}.

We also varied the initial monomer concentration with a PLA/PMMA composition ranging from 0/100 to 50/50 wt % for the system containing a $[AIBN]_0$ concentration of 7.5×10^{-2} mol L^{-1} and an initial MMA/DUDMA composition of 99/1 mol % (Figure 7). An earlier onset of the Trommsdorff effect occurred in the presence of increasing contents of PLA, considering the increase in the initial viscosity of the reaction medium caused by such a macromolecular diluent. At the beginning of the copolymerization process, the steady-state regime was verified, and the linear variation of the $(R_p)_0/[AIBN]_0^{1/2}$ vs $[M]_0$ plot (Figure 6b) showed that the external order of the reaction with respect to monomer was equal to 1. From the slope of this plot, we determined another value of k_{app} for the copolymerization process of MMA with DUDMA at 65 °C, in the presence of PLA oligomers: $k_{app} = (5.4 \pm 1.0) \times 10^{-2}$ $L^{1/2}$ $mol^{-1/2}$ min^{-1}. This value matched that determined above by varying AIBN concentration. Within the experimental errors, it can be concluded that such a k_{app} value was in reasonable agreement with that found for the DUDMA-containing single network formation.

4. Assessment of PLA Domain Sizes in Semi-IPNs by Turbidimetry. The turbidity τ is an intrinsic optical property of a material corresponding to the relative attenuation of light by the material. In the field of IPN-related materials,[28] the turbidity can be consid-

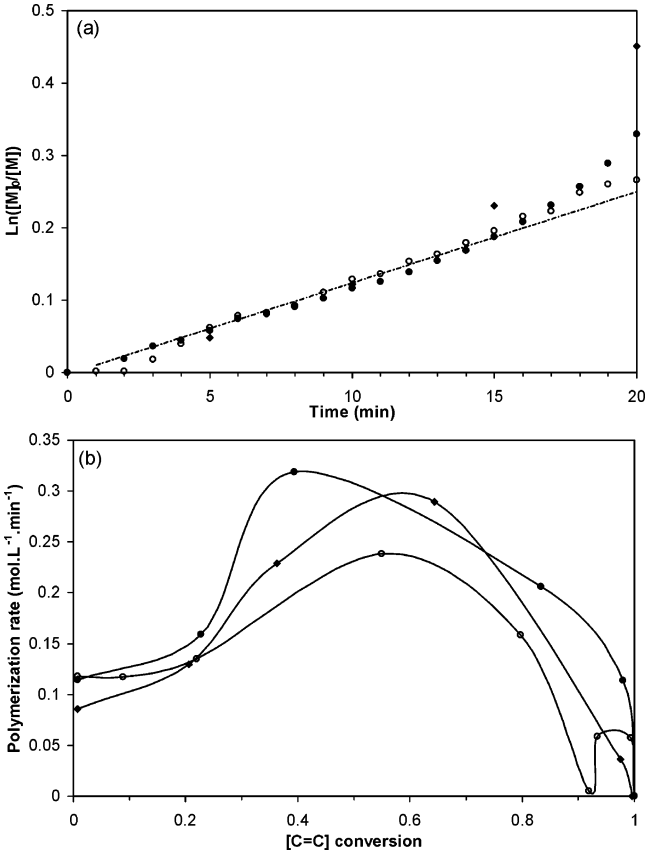

Figure 7. Influence of the PLA/PMMA composition on semi-IPN formation with $[AIBN]_0 = 7.5 \times 10^{-2}$ mol L^{-1} and an initial MMA/DUDMA composition of 99/1 mol %: (a) $\ln([M]_0/[M])$−time curves; (b) polymerization rate−conversion curves: ◆, 50/50 wt %; ●, 25/75 wt %; ○, 0/100 wt %.

ered as a meaningful parameter to assess the degree of chain interpenetration and the microdomain size, provided the difference between the refractive indices of both partners is significant. As a matter of fact, the experimental n_D^{25} values measured for the PLA oligomer and a PMMA sample—prepared under experimental conditions identical to those used for single network preparation—are 1.46 and 1.49, respectively. Considering that these n_D^{25} values are quite different, the transparency observed for some semi-IPN samples is at least indicative of microdomain sizes smaller than about 150 nm, according to Okay.[38]

It is noteworthy that both the cross-link density of the PMMA subnetwork and the cross-linker nature had a significant influence on the turbidity of semi-IPNs and obviously on the length scale of phase separation in these materials (Table 1). First, the microdomain sizes increased with the dimethacrylate content in the PMMA subnetwork. Indeed, the opaque semi-IPN with a 10 mol % BADMA content had a domain size larger than 150 nm, whereas the transparent sample with a 1 mol % BADMA content was characterized by a microdomain size smaller than 150 nm. These statements can be explained in terms of PLA/PMMA miscibility (cf. section 5). Second, for a given dimethacrylate content, the use of BADMA led to the creation of larger domains than those obtained when resorting to DUDMA. Indeed, the 5 mol % BADMA-containing semi-IPN was opaque, while its DUDMA-derivatized homologue was transparent. These interesting observations may mirror an enhanced miscibility between the PLA oligomer and DUDMA-based subnetworks due to the possibility of

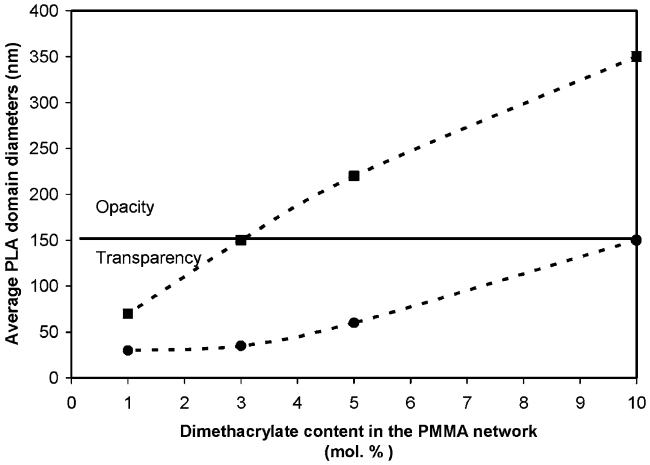

Figure 8. Average diameters of PLA domains in BADMA (■)- and DUDMA (●)-containing PLA/PMMA (50/50 wt %) semi-IPNs as determined by turbidimetry.

hydrogen bonding, as will be shown later (cf. section 5). It has to be stressed that the domain size in IPN-like structures can be controlled by two types of competitive factors: thermodynamic ones, i.e., intermolecular interactions between both partners, vs kinetic ones, i.e., competition between cross-linking and phase separation. Obviously enough, in the formation of PLA/PMMA semi-IPNs, the thermodynamic factors are predominant over the kinetic ones and are determining in the control of the extent of phase separation.

In a comparative study, we applied the theoretical expression derived by Blundell et al.[30] to our semi-IPN systems in order to estimate the average equivalent diameters of PLA microdomains (cf. Experimental Section, eq 4). Figure 8 shows the dependence of PLA domain diameter on dimethacrylate nature and content. Regardless of the dimethacrylate nature, the microdomain size increased with the cross-linker content in the PMMA subnetwork. On the other hand, for a given dimethacrylate content, the domain size was larger in the BADMA-containing semi-IPNs. Indeed, while all semi-IPN samples prepared from DUDMA were characterized by PLA diameters smaller than or equal to 150 nm, the BADMA-based homologues with an initial dimethacrylate content higher than 3 mol % possessed PLA diameters whose diameter was higher than 150 nm. Hence, both sets of results corroborated the conclusions inferred from the visual observations.

5. Evaluation of PLA/PMMA Interaction Parameters. To gain a better insight into the morphology developed in our semi-IPN systems, PLA/PMMA interaction parameters (χ) were evaluated between the PLA oligomer and either MMA/DUDMA or MMA/BADMA copolymer networks. Because relatively weak interactions (van der Waals forces or hydrogen bonds) are involved in the systems under study, the χ values can be related to the Hildebrand solubility parameters of both partners using eq 8:[39−42]

$$\chi = \frac{V_m}{RT}(\delta_1 - \delta_2)^2 \tag{8}$$

where V_m and T are the reference molar volume and the temperature, taken as 100 cm^3 mol^{-1} and 298 K, respectively, R is the gas constant, δ_1 is the solubility parameter of PLA, and δ_2 is the solubility parameter of a methacrylic copolymer network. δ_1 was calculated

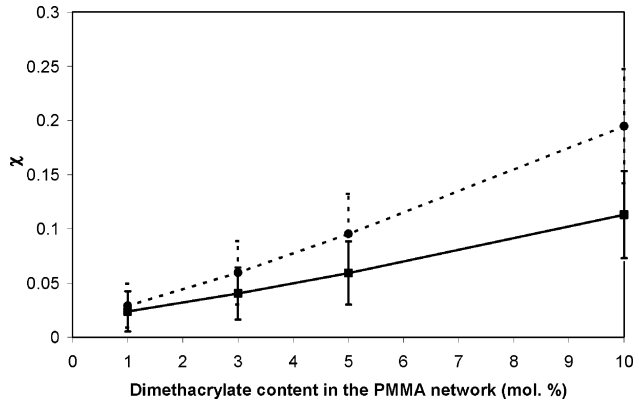

Figure 9. Dependence of PLA/PMMA interaction parameters on dimethacrylate content for BADMA (■)- and DUDMA (●)-containing PLA/PMMA (50/50 wt %) semi-IPNs.

using the group contribution method based on Van Krevelen's molar attraction constants:[42] $\delta_1 = 18.56$ $MPa^{1/2}$. δ_2 was calculated using an additive molar contribution relationship, as follows (eq 9):[43]

$$\delta_2\,(\mathrm{MPa}^{1/2}) = \frac{M_A F_A + M_B F_B}{M_A V_{m,A} + M_B V_{m,B}} \tag{9}$$

where M, V_m, and F are respectively the molar fraction, the molar volume of monomeric units, and the molar attraction constants associated with components A (PMMA) and B (BADMA or DUDMA).

The dependence of χ parameters on the dimethacrylate content for DUDMA- and BADMA-containing systems is plotted in Figure 9. It is noteworthy that the χ values increased with the cross-linker content. Accordingly, the extent of miscibility between PLA subchains and PMMA subnetworks decreased with increasing amounts of dimethacrylates, thus explaining the results obtained from semi-IPN turbidity.

To evaluate the influence of dimethacrylate nature on the miscibility of both semi-IPN partners, critical interaction parameters (χ_{cr}) were estimated for the systems considered. The χ_{cr} values were calculated from eq 10[39−42]

$$\chi_{cr} = \frac{1}{2}\left(\frac{1}{\sqrt{N_1}} + \frac{1}{\sqrt{N_2}}\right)^2 \tag{10}$$

where N_1 and N_2 are the polymerization degrees of PLA oligomer and PMMA subnetworks, respectively. When a polymer is cross-linked, N is equal to infinity; hence, the latter equation could simply be expressed as follows (eq 11):

$$\chi_{cr} = \frac{1}{2N_1} \tag{11}$$

Applying eq 11 to the PLA oligomer used in this investigation ($N_1 = 23$), the value of χ_{cr} was 0.021 ($\Delta\delta_{cr} = 0.47$ (cal $cm^{-3})^{1/2}$ with $V_m = 57.7$ cm^3 mol^{-1}). It has to be stressed that this value is valid for systems with only dispersive forces. According to Coleman's practical guide to polymer miscibility,[41] $\Delta\delta_{cr}$ can be increased by steps of 0.25 (cal $cm^{-3})^{1/2}$, depending on the strength of the potential intermolecular interactions present between the polymeric components of biphasic systems. Thus, $\Delta\delta_{cr}$ was increased from 0.47 to 0.72 (cal $cm^{-3})^{1/2}$ in BADMA-based semi-IPNs involving dipole−dipole interactions between ester groups from PLA and PMMA partners. The corresponding χ_{cr} value was equal to 0.05. It is noteworthy that $\chi > \chi_{cr}$ for BADMA contents higher than 3 mol %, suggesting a high degree of immiscibility in PLA/PMMA semi-IPNs with the latter dimethacrylate contents. This prediction matched the conclusions drawn from visual observations as well as DSC and turbidity measurements for BADMA-derivatized systems.

Table 3. Variation of χ_{cr} Parameters as a Function of DUDMA Content for PLA/PMMA Semi-IPNs

initial MMA/DUDMA composition (mol %)	χ_{cr}	$\chi_{cr} - \chi$
90/10	0.21	0.015
95/5	0.14	0.045
97/3	0.09	0.031
99/1	0.05	0.021

On the other hand, in DUDMA-based semi-IPNs, hydrogen bonding could potentially be established between the urethane functions of DUDMA cross-links and the main-chain ester groups of PLA oligomer. The extent of hydrogen bonding, so in turn the strength of intermolecular interactions, could be increased with increasing amounts of DUDMA. Therefore, $\Delta\delta_{cr}$ was further increased depending on the DUDMA content. The different χ_{cr} values estimated for DUDMA-containing semi-IPNs are reported in Table 3. These values increased significantly with DUDMA content. Interestingly, the χ values were smaller than the corresponding χ_{cr} ones ($\chi_{cr} - \chi > 0$), indicating a high extent of miscibility in all prepared PLA/PMMA semi-IPNs using DUDMA as the cross-linker. The length scale of phase separation in such semi-IPNs was thus restricted to domain sizes smaller than about 150 nm because of the presence of highly favorable hydrogen bonds. Again, the calculation of PLA/PMMA interaction parameters and the comparison between χ and χ_{cr} values may well account for our previous results.

6. Design of Porous Networks from Semi-IPNs. Porous methacrylic networks were readily obtained by mere extraction of un-cross-linked PLA oligomers from PLA/PMMA semi-IPNs. It is important to stress that such a quantitative extraction was performed with a good solvent of PLA at a temperature (40 °C) far below the T_g value of PMMA networks to avoid the collapse of the residual porous structures.[26a] The morphologies of semi-IPNs, before and after extraction, were examined by SEM (Figure 10). Whatever the cross-link density and the cross-linker nature, the nonextracted samples displayed compact structures without any pore. The corresponding PMMA single networks, after extraction, did not exhibit any pore either, indicating a high compacity in this type of networks. In sharp contrast, the morphology exhibited by extracted semi-IPNs was dramatically different, despite an identical chemical structure. The micrographs of the latter samples revealed highly porous structures, thus showing the effective role of PLA oligomer as a template porogen. Pore sizes strongly depended on the dimethacrylate nature and content. Indeed, pore diameters ranged from 50 to 400 nm for the 10 mol % BADMA-containing network and from 25 to 175 nm for its DUDMA-based homologue. Moreover, pore size decreased significantly when decreasing the cross-linker content (Table 4). The dependence of pore size in such nanoporous materials actually mirrored the differences observed in semi-IPN precursors from visual aspects, turbidity measurements,

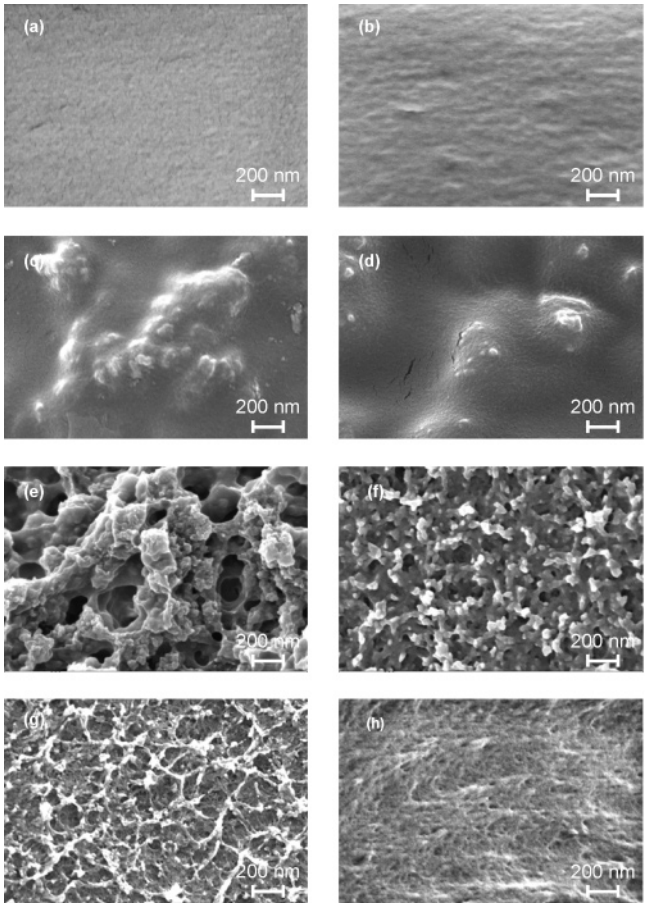

Figure 10. SEM micrographs of different networks. PMMA single networks after extraction: (a) 10 mol % DUDMA-based sample, (b) 1 mol % DUDMA-based sample; PLA/PMMA (50/50 wt %) semi-IPNs: (c) 10 mol % BADMA-based nonextracted sample, (d) 10 mol % DUDMA-based nonextracted sample, (e) 10 mol % BADMA-based sample after extraction, (f) 10 mol % DUDMA-based sample after extraction, (g) 1 mol % BADMA-based sample after extraction, (h) 1 mol % DUDMA-based sample after extraction.

Table 4. PLA Domain Diameters of Semi-IPNs As Determined by Turbidimetry and Pore Diameters of Resulting Porous Networks As Determined by SEM and Thermoporometry

initial MMA/dimethacrylate composition (mol %)	av PLA domain diam turbidimetry (nm)	pore diam SEM (nm)	pore diam thermoporometry (nm)
MMA/BADMA			
90/10	350	50−400	10−200[a]
95/5	220	20−300	15−200[a]
97/3	150	10−150	10−150
99/1	70	10−100	30−70
MMA/DUDMA			
90/10	150	25−175	20−170
95/5	60	25−75	10−95
97/3	35	20−60	30−80
99/1	30	10−50	30−65

[a] Thermoporometry only allowed for determination of pore size up to 200 nm. For larger pore sizes, the melting peaks of confined and bulk water were not resolved: confined water just behaved as a bulk solvent.

and polymer−polymer miscibility inferred from the calculation of PLA/PMMA interaction parameters.

Thermoporometry has proved to be a reliable technique for the determination of pore size distributions in a wide range of (meso)porous materials, including

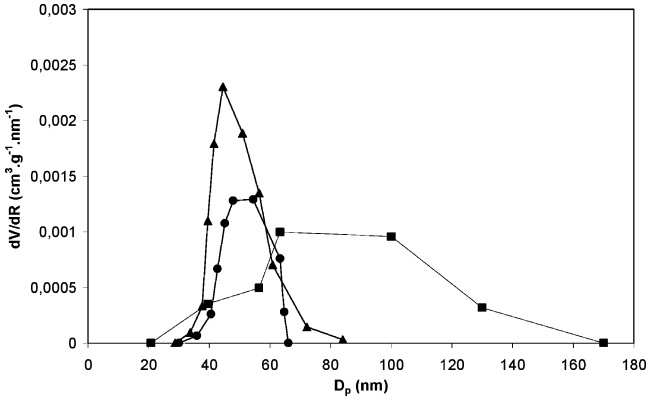

Figure 11. Pore size distribution profiles of porous methacrylic networks as determined by thermoporometry for PLA/PMMA (50/50 wt %) semi-IPN systems containing different initial MMA/DUDMA compositions: ■, 10 mol %; ▲, 3 mol %; ●, 1 mol %.

porous silica, cellulose membranes, and hydrogels.[31] We thus determined pore sizes of the porous methacrylic networks by this interesting technique through DSC measurements using water as the penetrant solvent (cf. Experimental Section, eqs 5 and 6). The pore size ranges thus obtained are reported in Table 4, and examples of pore size distributions are shown in Figure 11. It is noteworthy that pore size distributions were narrower for DUDMA-containing systems. This arises from the enhanced miscibility between both partners in DUDMA-based semi-IPN precursors, as explained in the previous section. Overall, the results of pore sizes obtained by SEM and thermoporometry were in reasonable agreement; they were also in agreement with the average values of PLA domain diameters as determined by turbidimetry for semi-IPN precursors. SEM and thermoporometry analyses turned out to be complementary as the former technique was more appropriate to characterize the largest pore sizes (>200 nm), while the latter one was more precise to determine the smallest pore diameters (<200 nm).

It is interesting to point out that the density values of extracted semi-IPNs—as determined by pycnometry—were very close to those of corresponding single networks. For instance, the 10 and 1 mol % DUDMA-containing semi-IPNs had density values at 25 °C equal to 1.204 and 1.150, respectively, and the values of density for the corresponding single networks were 1.202 and 1.183, respectively. This strongly indicates that the porous networks observed by SEM were monolithic structures constituted of open pores or interconnected channels through which a fluid (water or helium) could circulate. The density of a porous PMMA network (around 1.2) actually corresponds to the density of the PMMA matrix, i.e., the true density. Moreover, the porous samples were wrapped in a polyethylene film and placed in *n*-pentane ($d_{20°C}$ = 0.62[44]): in such a low-density solvent, they did float, suggesting an apparent density as well as a porosity ratio lower than or equal to values around 0.6. Such values were in agreement with those expected, taking into account the quantitative extraction of linear PLA from semi-IPNs with a 50/50 wt % PLA/PMMA composition.

Conclusions

As highlighted in the Introduction, the use of an organic solvent as a porogen in free-radical cross-linking

reactions provides an easy and practical method for preparing porous polymeric materials. However, the final products generally have a broad pore size distribution ranging from micropores to macropores, and the polymer properties and morphologies strongly depend on the experimental conditions used (stirring, temperature, time, suspension or bulk polymerization technique, etc.). Moreover, much progress has been recently achieved toward engineering nanoporous polymers with a defined porosity. Miscellaneous approaches are now applied by selectively removing single polymer domains from macromolecular architectures. In this context, low-polydispersity block copolymers with one selectively removable block constitute original precursors. Nevertheless, their synthesis may be quite costly, and their utilization for the generation of mesoporous polymer structures with suitable mechanical and morphological stability generally requires cross-linking of the remaining block.

This report demonstrates the versatility and effectiveness of the extraction of un-cross-linked oligoesters from PLA/PMMA-based semi-IPNs as a straightforward and alternative strategy for generating macro- to mesoporous networks. Un-cross-linked PLA subchains may well serve as porogen templates for the design of such porous polymeric materials. Thanks to the calculation of χ parameters for PLA/PMMA systems, the dependence of pore sizes and pore size distributions on the dimethacrylate content and nature can be explained in terms of polymer−polymer miscibility in semi-IPN precursors. In other words, the pore size can be tuned by varying these structural parameters through the variation of miscibility between the PLA oligomer and the PMMA subnetwork. A decrease in the cross-linker content leads to a decrease in PLA domain sizes, so in turn pore sizes decrease and pore size distributions are narrower. Moreover, because of the presence of highly favorable hydrogen bonds in DUDMA-derivatized semi-IPNs, the extent of miscibility between both partners is enhanced, and PLA domain sizes are smaller than 150 nm up to a 10 mol % DUDMA content: the resulting porous networks are characterized by relatively narrow pore size distributions. The influence of the oligoester nature and molar mass in semi-IPNs on the porosity associated with the porous networks derived therefrom as well as the utilization of IPNs constituted of polyester and PMMA subnetworks as precursors for the generation of mesoporous materials will be published in forthcoming papers.

These versatile approaches involving semi-IPN and IPN systems may provide an easy way to control the morphology associated with porous networks and to functionalize the pore surface by initial incorporation of functional monomers. We believe that such porous materials may find potential applications in separation techniques as chromatography supports, as well as membrane catalysis, and more generally in chemistry in confined medium as nanoreactors.

Acknowledgment. The "Région Ile-de-France" Council is gratefully acknowledged for financial support through SESAME projects allowing for the purchase of SEM and solid-state NMR equipments. The authors thank the French Ministry of Research for providing G.R. with a grant. They are also indebted to Dr. J. L. Pastol (CNRS, Vitry-sur-Seine, France) for his cooperation in SEM analyses as well as to C. Gaillet and G. Da Costa for their kind technical assistance.

References and Notes

(1) Tavolaro, A.; Drioli, E. *Adv. Mater.* **1999**, *11*, 975.
(2) Dunleavy, M. J. *Med. Device Technol.* **1996**, *5*, 14.
(3) Svec, F.; Peters, E. C.; Sykora, D.; Yu, C.; Fréchet, J. M. J. *J. High Resolut. Chromatogr.* **2000**, *23*, 3.
(4) Martin, C. R. *Science* **1994**, *266*, 1961.
(5) Hentze, H. P.; Antonietti, M. *Rev. Mol. Biotech.* **2002**, *90*, 27.
(6) Sing, K. S. W.; Everett, D. H.; Haul, R. A. W.; Moscou, L.; Pierotti, J.; Rouquerol, J.; Siemieniewska, T. *Pure Appl. Chem.* **1985**, *57*, 603.
(7) Balaji, R.; Boileau, S.; Guérin, Ph.; Grande, D. *Polym. News* **2004**, *29*, 205.
(8) Wulff, G. *Chem. Rev.* **2002**, *102*, 1.
(9) Haupt, K.; Mosbach, K. *Trends Biotechnol.* **1998**, *16*, 468.
(10) (a) Maki-Ontto, R.; de Moel, K.; de Odorico, W.; Ruokolainen, J.; Stamm, M.; ten Brinke, G.; Ikkala, O. *Adv. Mater.* **2001**, *13*, 117. (b) De Moel, K.; Alberda van Ekenstein, G. O. R.; Nijland, H.; Polushkin, E.; ten Brinke, G.; Maki-Ontto, R.; Ikkala, O. *Chem. Mater.* **2001**, *13*, 4583. (c) Ikkala, O.; ten Brinke, G. *Science* **2002**, *295*, 2407.
(11) Lee, J. S.; Hirao, A.; Nakahama, S. *Macromolecules* **1988**, *21*, 274.
(12) Hashimoto, T.; Tsutsumi, K.; Funaki, Y. *Langmuir* **1997**, *13*, 6869.
(13) (a) Park, M.; Harrison, C.; Chaikin, P. M.; Register, R. A.; Adamson, D. H. *Science* **1997**, *276*, 1401. (b) Li, R. R.; Dapkus, P. D.; Thompson, M. E.; Jeong, W. G.; Harrison, C.; Chaikin, P. M.; Register, R. A.; Adamson, D. H. *Appl. Phys. Lett.* **2000**, *76*, 1689.
(14) (a) Hedrick, J. L.; Carter, K. R.; Richter, R.; Miller, R. D.; Russell, T. P.; Flores, V.; Mecerreyes, D.; Dubois, P.; Jérôme, R. *Chem. Mater.* **1998**, *10*, 39. (b) Mansky, P.; DeRouchey, J.; Russell, T. P.; Mays, J.; Pitsikalis, M. Morkved, T.; Jaeger, H. *Macromolecules* **1998**, *31*, 4399. (c) Thurn-Albrecht, T.; DeRouchey, J.; Russell, T. P.; Jaeger, H. *Macromolecules* **2000**, *33*, 3250. (d) Thurn-Albrecht, T.; Steiner, R.; DeRouchey, J.; Stafford, C. M.; Huang, E.; Bal, M.; Tuominen, M.; Hawker, C. J.; Russell, T. P. *Adv. Mater.* **2000**, *12*, 787. (e) Xu, T.; Kim, H. C.; DeRouchey, J.; Seney, C.; Levesque, C.; Martin, P.; Stafford, C. M.; Russell, T. P. *Polymer* **2001**, *42*, 9091. (f) Thurn-Albrecht, T.; DeRouchey, J.; Russell, T. P.; Kolb, R. *Macromolecules* **2002**, *35*, 8106. (g) Xu, T.; Hawker, C. J.; Russell, T. P. *Macromolecules* **2003**, *36*, 6178.
(15) Liu, G. J.; Ding, J. F.; Hashimoto, T.; Kimishima, K.; Winnik, F. M.; Nigam, S. *Chem. Mater.* **1999**, *11*, 2233.
(16) Chan, V. Z. H.; Hoffman, J.; Lee, V. Y.; Iatrou, H.; Avgeropoulos, A.; Hadjichristidis, N.; Miller, R. D.; Thomas, E. L. *Science* **1999**, *286*, 1716.
(17) (a) Zalusky, A. S.; Olayo-Valles, R.; Taylor, C. J.; Hillmyer, M. A. *J. Am. Chem. Soc.* **2001**, *123*, 1519. (b) Olayo-Valles, R.; Wolf, J. *J. Am. Chem. Soc.* **2002**, *124*, 12761. (c) Cavicchi, K. A.; Zalusky, A. S.; Hillmyer, M. A.; Lodge, T. P. *Macromol. Rapid Commun.* **2004**, *25*, 704.
(18) Li, M.; Douki, K.; Goto, K.; Li, X.; Coenjarts, C.; Smilgies, D. M.; Ober, C. K. *Chem. Mater.* **2004**, *16*, 3800.
(19) (a) Hedrick, J. L.; Miller, R. D.; Hawker, C. J.; Carter, K. R.; Volksen, W.; Yoon, D. Y.; Trollsas, M. *Adv. Mater.* **1998**, *10*, 1049. (b) Hedrick, J. L.; Carter, K. R.; Labadie, J. W.; Miller, R. D.; Volksen, W.; Hawker, C. J.; Yoon, D. Y.; Russell, T. P.; McGrath, J. E.; Briber, R. M. *Adv. Polym. Sci.* **1999**, *141*, 1. (c) Nguyen, C.; Hawker, C. J.; Miller, R. D.; Huang, E.; Hedrick, J. L.; Gauderon, R.; Hilborn, J. G. *Macromolecules* **2000**, *33*, 4281.
(20) Eigner, M.; Voit, B.; Estel, K.; Bartha, J. W. *e-Polym.* **2002**, 028.
(21) Loera, A. G.; Cara, F.; Dumon, M. Pascault, J. P. *Macromolecules* **2002**, *35*, 6291.
(22) Buchmeiser, M. R. *Angew. Chem., Int. Ed.* **2001**, *40*, 3795.
(23) (a) Widmaier, J. M.; Sperling, L. H. *Macromolecules* **1982**, *15*, 625. (b) Widmaier, J. M.; Sperling, L. H. *Br. Polym. J.* **1984**, *16*, 46.
(24) Du Prez, F.; Goethals, E. J. *Macromol. Chem. Phys.* **1995**, *196*, 903.
(25) Kayaman-Apohan, N.; Baysal, B. M. *Macromol. Chem. Phys.* **2001**, *202*, 1182.
(26) (a) Grande, D.; Pastol, J. L.; Guérin, Ph.; Boileau, S. *Polym. Prepr.* (*Am. Chem. Soc., Div. Polym. Chem.*) **2003**, *44* (1), 44.

(b) Grande, D.; Lacoudre, N.; Guérin, Ph.; Boileau, S. *Polym. Prepr.* (*Am. Chem. Soc., Div. Polym. Chem.*) **2003**, *44* (1), 148.
(27) (a) Hu, J.; Pompe, G.; Schulze, U.; Pionteck, J. *Polym. Adv. Technol.* **1998**, *9*, 746. (b) Hu, J.; Schulze, U.; Pionteck, J. *Polymer* **1999**, *40*, 5279. (c) Pionteck, J.; Hu, J.; Schulze, U. *J. Appl. Polym. Sci.* **2003**, *89*, 1976.
(28) (a) Sperling, L. H. In *Interpenetrating Polymer Networks and Related Materials*; Plenum Press: New York, 1981. (b) *Interpenetrating Polymer Networks*; Klempner, D., Sperling, L. H., Utracki, L. A., Eds.; Advances in Chemistry Series 239; American Chemical Society: Washington, DC, 1994. (c) Sperling, L. H.; Mishra, V. *Polym. Adv. Technol.* **1996**, *7*, 197.
(29) Bachari, A.; Bélorgey, G.; Hélary, G.; Sauvet, G. *Macromol. Chem. Phys.* **1995**, *196*, 411.
(30) Blundell, D. J.; Longman, G. W.; Wignall, G. D.; Bowden, M. J. *Polymer* **1974**, *15*, 33.
(31) (a) Brun, M.; Lallemand, A.; Quinson, J.-F.; Eyraud, C. *Thermochim. Acta* **1977**, *21*, 59. (b) Iza, M.; Woerly, S. Danumah, C.; Kaliaguine, S.; Bousmina, M. *Polymer* **2000**, *41*, 5885. (c) Hay, J. N.; Laity, P. R. *Polymer* **2000**, *41*, 6171.
(32) Lu, H.; Lovell, L. G.; Bowman, C. N. *Macromolecules* **2001**, *34*, 8021.
(33) Eguiburu, J. L.; Iruin, J. J.; Fernandez-Berridi, M. J.; San Roman, J. *Polymer* **1998**, *39*, 6891.
(34) Jin, S. R.; Widmaier, J. M.; Meyer, G. C. *Polymer* **1988**, *29*, 346.
(35) Hill, D. J. T.; O'Donnell, H. J.; Pomery, P. J. *Eur. Polym. J.* **1997**, *33*, 1353.
(36) Laskar, J.; Vidal, F.; Fichet, O.; Gauthier, C.; Teyssié, D. *Polymer* **2004**, *45*, 5047.
(37) (a) Masson, J. C. In *Polymer Handbook*, 3rd ed.; Brandrup, J., Immergut, E. H., Eds.; Wiley-Interscience: New York, 1989; p II/3. (b) Berger, K. C.; Meyerhoff, G. In *Polymer Handbook*, 3rd ed.; Brandrup, J., Immergut, E. H., Eds.; Wiley-Interscience: New York, 1989; p II/73.
(38) Okay, O. *Prog. Polym. Sci.* **2000**, *25*, 711.
(39) Klein, P. G.; Ebdon, J. R.; Hourston, D. J. *Polymer* **1988**, *29*, 1079.
(40) Grulke, E. A. In *Polymer Handbook*, 3rd ed.; Brandrup, J., Immergut, E. H., Eds.; Wiley-Interscience: New York, 1989; p VII/525.
(41) Coleman, M. M.; Serman, C. J.; Bhagwagar, D. E.; Painter, P. C. *Polymer* **1990**, *31*, 1187.
(42) Van Krevelen, D. W. In *Properties of Polymers*; Elsevier: Amsterdam, 1997.
(43) Lee, J.-C.; Litt, M. H.; Rogers, C. E. *Macromolecules* **1998**, *31*, 4232.
(44) *Handbook of Chemistry and Physics*, 55th ed.; Weast, R. D., Ed.; CRC Press: Cleveland, OH, 1974; p C-407.

MA0501390